

Article

Not peer-reviewed version

---

# Preparation and Properties of a Novel Nylon 6 Co-polymerized by $\varepsilon$ -Caprolactam and $\alpha$ -Amino- $\varepsilon$ -Caprolactam

---

[Xiaoyu Mao](#) , Wei Liu , Shan Mei , Zeyang Li , [Baoning Zong](#) \*

Posted Date: 18 April 2024

doi: 10.20944/preprints202404.1185.v1

Keywords: Hydrolysis open-ring polymerization; Modified branched PA6; Thermal properties; Rheological properties; Mechanical properties



Preprints.org is a free multidiscipline platform providing preprint service that is dedicated to making early versions of research outputs permanently available and citable. Preprints posted at Preprints.org appear in Web of Science, Crossref, Google Scholar, Scilit, Europe PMC.

Copyright: This is an open access article distributed under the Creative Commons Attribution License which permits unrestricted use, distribution, and reproduction in any medium, provided the original work is properly cited.

Disclaimer/Publisher's Note: The statements, opinions, and data contained in all publications are solely those of the individual author(s) and contributor(s) and not of MDPI and/or the editor(s). MDPI and/or the editor(s) disclaim responsibility for any injury to people or property resulting from any ideas, methods, instructions, or products referred to in the content.

Article

# Preparation and Properties of a Novel Nylon 6 Co-Polymerized by $\epsilon$ -Caprolactam and $\alpha$ -Amino- $\epsilon$ -Caprolactam

Xiaoyu Mao <sup>1</sup>, Wei Liu <sup>1</sup>, Zeyang Li <sup>1</sup>, Shan Mei <sup>2</sup> and Baoning Zong <sup>3,\*</sup>

<sup>1</sup> Research Center of Renewable Energy, Research Institute of Petroleum Progressing, SINOPEC, Beijing 100083, China.

<sup>2</sup> NO.22 Research Department, Research Institute of Petroleum Progressing, SINOPEC, Beijing 100083, China.

<sup>3</sup> State Key Laboratory of catalytic Material and Reaction Engineering, Research Institute of Petroleum Progressing, SINOPEC, 18<sup>th</sup> Xueyuan Road, Haidian District, Beijing 100083, China.

\* Correspondence: zongbn.ripp@sinopec.com

**Abstract:** In this study, we successfully synthesized a novel branched polyamide 6 with  $\epsilon$ -caprolactam(CPL) and  $\alpha$ -Amino- $\epsilon$ -caprolactam(ACL) through hydrolytic ring-open co-polymerization. The NMR characterization and rheological test result proved the existence of branched chain structure additionally. The branched chain structure caused a remarkable enhancement in the rheological properties. The met index(MFR),zero shear rate viscosity and storage modulus at low frequency region had a remarkable increase. The shear thinning phenomenon became more obvious. The thermal properties test determined by differential scanning calorimetry(DSC) showed that the melting point and crystallinity of co-polymers decreased with the increase of ACL addition. However, the crystal structure of the samples remained unchanged. The appropriate addition amount of ACL can improve the tensile mechanical properties of the co-polymers. When the amount of ACL was 1%, the tensile strength and fracture elongation rate of the co-polymers had the most significant increase.

**Keywords:** hydrolysis open-ring polymerization; modified branched PA6; thermal properties; rheological properties; mechanical properties

## 1. Introduction

Polyamide 6 (PA6), also known as nylon 6, is a kind of high-performance polymer with processability, excellent mechanical properties, chemical durability, and low cost. It can be used for spinning, blow molding, and industrial molding, which contributes to a wide range of applications in the fields of textiles, packaging, and engineering plastics.[1-3] Currently, industrial nylon 6 is mostly prepared by hydrolysis ring-opening polymerization of  $\epsilon$ -caprolactam(CPL) at high temperature, which has the advantages of relatively mild reaction conditions, easy scale-up production, and narrow molecular weight distribution. However, due to the influence of the hydrolysis ring-opening chemical equilibrium, the molecular weight of industrial nylon 6 products is not high.[1,4] Linear nylon 6 with not high molecular weight has insufficient melt strength, which limits its application in thermal forming, injection molding, foaming, and other fields dominated by stretching flow. [5] In addition, linear nylon 6 with not high molecular weight is highly sensitive to crack propagation and exhibits brittle fracture behavior under low temperature and severe load conditions, with poor impact resistance. [6] By introducing multifunctional monomers into the polymerization process, branched nylon 6 co-polymerized with the monomers and CPL can be prepared. Compared with linear nylon 6, branched nylon 6 has significantly different melt rheological properties and crystallization properties, which affect its processing properties in spinning, film stretching, injection molding, and other processes, thereby expanding the application of nylon 6.[7,8]

$\epsilon$ -lysine, with one carboxyl group and two amino groups, is an AB<sub>2</sub>-type multifunctional compound. Currently,  $\epsilon$ -lysine is mainly produced through fermentation of corn stalks in the industry, which has the advantages of wide raw material sources and environmental friendliness. [9] By co-polymerizing  $\epsilon$ -lysine or its derivatives with CPL, novel nylon 6 polymers with branched



structure can be obtained. Scholl et al.[10] prepared highly branched nylon 6 with a relative molecular weight of 23000 by starting from  $\epsilon$ -lysine salt and adding a certain amount of copolymerizable monomer and adjusting the polymerization conditions. Steeman et al. prepared randomly branched nylon 6 by copolymerizing 2,4,6-triaminohexanoic acid with CPL, and the long-chain branching led to an increase in the zero-shear viscosity of nylon 6 and a more pronounced shear-thinning behavior, while the melt strength increased. Li et al. [12] directly copolymerized  $\epsilon$ -lysine with CPL to prepare randomly branched nylon 6 with a small amount of long-chain branching. With the close relative viscosity, the melting point of long-chain branched nylon 6 is basically the same as that of linear nylon 6, and it exhibits a more significant shear-thinning phenomenon. The introduction of long-chain branching increases the entanglement between molecular chains, making the molecular chains more easily oriented along the processing direction.

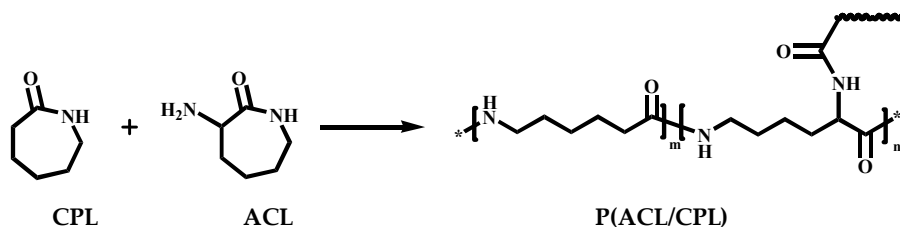


**Figure 1.** The co-polymerization of CPL and ACL.

In our previous work, we successfully synthesized  $\alpha$ -Amino- $\epsilon$ -caprolactam (ACL) by cyclizing lysine.[13] ACL has a similar structure to CPL, but amino group at the  $\alpha$  position contributes to bifunctionality after hydrolysis. In this study, we copolymerized CPL and ACL through hydrolytic ring-opening polymerization at different ACL/CPL ratios, and successfully prepared a modified nylon 6, named P(ACL/CPL), with long-chain branched structure(Scheme 1). The structure of P(ACL/CPL) was characterized by  $^1\text{H}$  NMR and  $^{13}\text{C}$  NMR spectra, which confirmed the feasibility of copolymerization and the generation of branched structures, and predicted the reaction mechanism. The rheological properties of the P(ACL/CPL) copolymer was tested using the rotational rheometer, and its thermodynamic characteristics were determined using the differential scanning calorimetry (DSC). Finally, the tensile behavior of P(ACL/CPL) was tested, and the optimal ratio of caprolactam to ACL was determined based on the results of rheological and thermodynamic tests.

## 2. Materials and Methods

### 2.1. Materials

The CPL used in this study was supplied by Baling Petrochemical Company, SINOPEC and the ACL was synthesized in our earlier work. Sulfuric acid and 2,2,2-Trifluoroethanol was purchased from Acros. The hydrochloric acid ethanol standard solution and potassium hydroxide ethanol standard solution used in this study were provided by Alfa.

### 2.2. Co-Polymerization of CPL and ACL

A certain ratio of CPL, ACL, and water were added to the 5L autoclave. Vacuuming was applied at room temperature until the pressure in autoclave reached -0.05MPa, then  $\text{N}_2$  gas was inflated to relieve vacuum. This vacuuming-inflation cycle was repeated 3 times, and finally inflating  $\text{N}_2$  gas to make the pressure in autoclave reach around 0.05MPa. The temperature was initially set at 225°C, and stirring was started at 100°C. After pre-polymerizing at 225°C for 0.5 hours, the temperature was raised to 245°C and maintained for 3 hours under pressure. The pressure was then released to atmospheric pressure, and the reaction was continued for another 1 hour. Finally, vacuuming was applied until the pressure reaches below -0.05MPa, and the reaction was continued for 1 hour. The product was then discharged and cut into pellets. The pelleted co-polymer was dissolved in 90°C hot water in order to remove the residual monomers and low molecular weight polymers.

### 2.3. Injection Molding of Co-Polymer

The prepared co-polymer was dried in a vacuum oven at 60°C for 12 hours to remove the absorbed moisture in the air. The barrel temperature of the injection molding machine(MiniJet Pro, Thermo Fisher Sci.) was set to 240°C, and the temperature of the mold cavity was set to 100°C. The injection time was 15 seconds and the injection pressure was 800 bar. The holding time was 10 seconds, and the holding pressure was 650 bar.

### 2.4. Characterization

The relative viscosity( $\eta_r$ ), intrinsic viscosity( $[\eta]$ ), and viscosity-average molecular weight of the co-polymer were determined by using a Ubbelohde viscometer. The copolymer was dissolved in a 96wt% sulfuric acid solution (solute:solvent, 1g:100mL). The time it took for the solvent and co-polymer solution to pass through the capillary at 25°C was measured by using the Ubbelohde viscometer. The molecular weight of the copolymer was calculated using the Mark-Houwink equation  $[\eta]=k[M_w]^a$ . The Mark-Houwink constants for nylon-6 in a 25°C, 96% sulfuric acid solution are  $k=6.3\times 10^{-4}$  and  $a=0.764$ .[1]

The end-group content of the co-polymer was tested by using a potentiometric titrator (Metrohm 916T-touch)according to GB/T 38138-2019. The co-polymer was dissolved in 88% trifluoroethanol solution at 60°C. First, 0.02 mol/L hydrochloric acid-ethanol standard solution was used to titrate the polymer solution cooled to 25°C, and a blank test was performed. Then, 0.02 mol/L potassium hydroxide-ethanol standard solution was used to titrate the solution that had just undergone amino concentration titration, with the titration process first neutralizing the excess hydrochloric acid and then titrating to the endpoint.

The structures of the resultant nylon-6 polymers were investigated by <sup>1</sup>H NMR and <sup>13</sup>C NMR (Becker AVANCE NEO 500M), using formic acid/trifluoroacetic acid-d (1:1, v:v) as the solvent.

The rheological properties of the samples were measured by using a rotational rheometer (HAAKE MARS P25CSL). The test specimens were prepared by injection molding with a diameter of 20mm and a thickness of 1mm. A frequency sweep was performed under oscillatory mode with a strain of 1% and a frequency range of 0.1-500rad/s to obtain the variation of complex viscosity ( $\eta$ ), storage modulus ( $G'$ ) and loss modulus ( $G''$ ) with angular frequency ( $\omega$ ). The melt flow index of the copolymer was determined using a melt flow indexer (Thermo Scientific) at a testing pressure of 2.16kg and a chamber temperature of 230°C.

The thermal properties of the co-polymers were determined by differential scanning calorimetry (DSC, DSC3 METLER TOLEDO). Under N<sub>2</sub> atmosphere the samples was first heated from 25°C to 300°C to remove thermal history, with a heating rate of 20°C/min. Then, at a cooling rate of 10°C/min the samples were cooled from 300°C to 25°C to test their crystallization performance. Finally, the samples were heated from 25°C to 300°C at a heating rate of 10°C/min to test their melting performance. The degree of crystallinity( $X_c$ ) was obtained by Equation1.

$$X_c = \Delta H_m / \Delta H_0 \times 100\% \quad (1)$$

where  $\Delta H_m$  is the specific enthalpy of melting, and  $\Delta H_0$  is the enthalpy of melting with 100% crystalline nylon 6 (188 J/g )[14].The crystal type of the sample was tested using an X-ray diffractometer, with a scanning range of 5° to 50° and a scanning speed of 2 °/min.

The tensile mechanical properties were checked by the universal tensile machine (MTS/SANS CMT2000) according to ASTM D638. The strain rate was 10 mm/min.

All of those specimens were kept in a desiccator under vacuum for 24 hbefore the measurements

## 3. Results

The reaction mechanism of nylon 6 synthesis via hydrolytic ring-opening polymerization of caprolactam is well-understood. Under high temperature and water conditions, the amide bond of caprolactam undergoes cleavage, resulting in the formation of aminocaproic acid(Figure 2(a)). Aminocaproic acid can undergo condensation to form short-chain polyamide. The terminal amino group of the short-chain polyamide attacks the carbonyl carbon of the CPL monomer's amide bond, directly adding the CPL monomer to the polymer chain and achieving chain growth. [29] For our co-polymer system, the reaction progress and mechanism can be shown in Figure 2. ACL was supposed to have the similar properties to CPL so that its amide bond can also cleavage to form linear

molecule(Figure 2(b)). A small account of ring opening products of CPL and ACL can undergo polycondensation to form low molecular weight polymers with main chain and side chain(Figure 2(c)). The terminal amino groups in both main chain and side chain of the polymer can react with the monomers protonated by carboxyl groups leading to chain addition(Figure 2(d)).

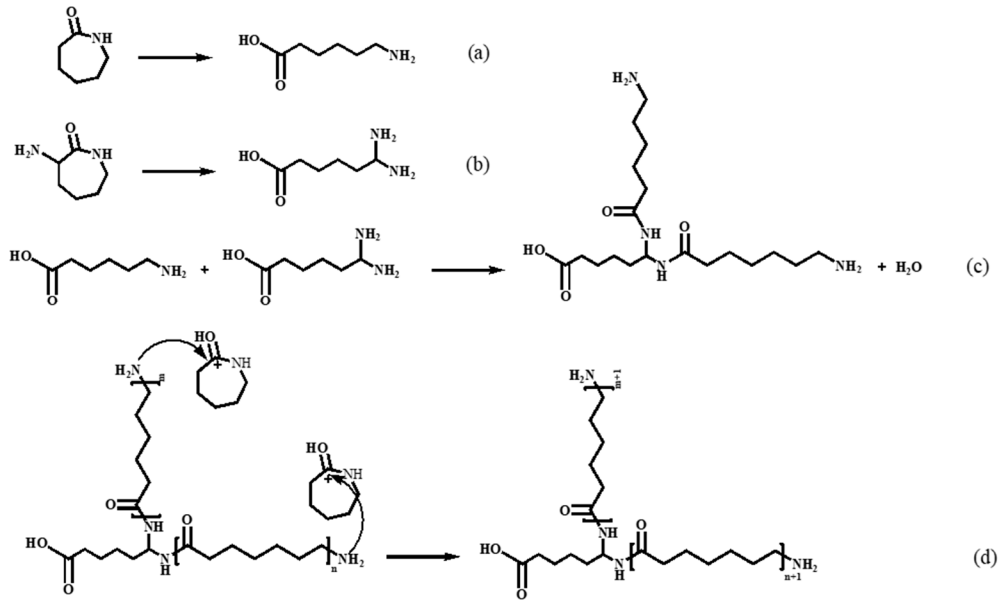


**Figure 2.** The reaction mechanism of CPL and ACL:(a)The open-ring of CPL;(b)The open-ring of ACL;(c)The polycondensation of open-ring products;(d)The chain addition.

The chemical shifts of H atoms and C at branching sites were determined by <sup>1</sup>H NMR and <sup>13</sup>C NMR, respectively, to determine the structure of the P(ACL/CPL) co-polymer. The structural formula and <sup>1</sup>H NMR spectrum of P(ACL/CPL) are shown in Figure 3(a), with the chemical shifts of H atoms as follows: δ4.63 (branching site), δ3.42, 2.58, 1.45-1.78 (main chain and side chain). The structural formula and <sup>13</sup>C NMR spectrum of P(ACL/CPL) are given in Figure 3(b), with the chemical shifts of C atoms as follows: δ65.2 (branching site), δ3.42, 2.58, 1.45-1.78 (main chain and side chain).

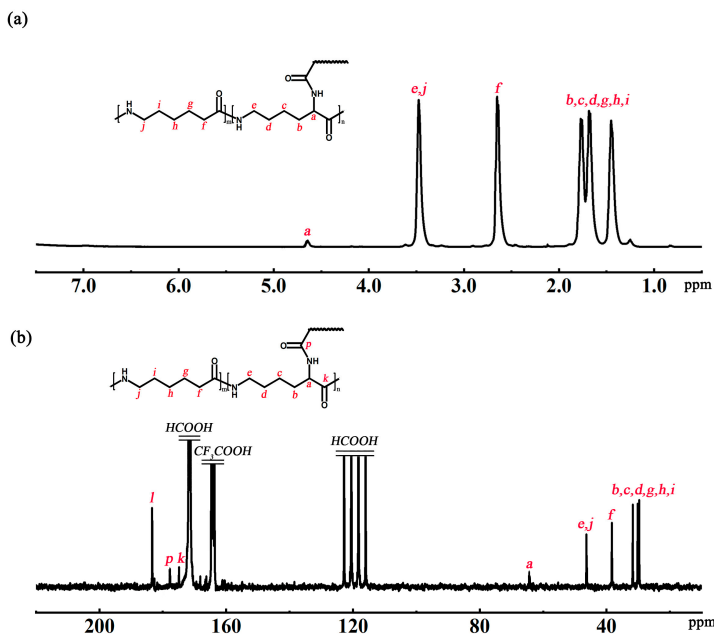


**Figure 3.** The <sup>1</sup>H NMR spectra(a) and the <sup>13</sup>C NMR spectra(b) of P(ACL/CPL).

The rheological properties of polymers, highly sensitive to the changes in molecular chain, can be used to reveal chain structure of polymers.[15] The complex viscosity ( $\eta$ ) of pure PA6 and our co-polymer samples as a function of angular frequency ( $\omega$ ) is shown in Figure 4. With linear molecular chain structure, pure PA6 complex viscosity showed little change with angular frequency increased, and the the  $\eta$ - $\omega$  curve of which showed a clear Newtonian plateau. After the addition of ACL, the complex viscosity of the co-polymers decreased significantly with the increase of angular frequency, and the Newtonian plateau in the  $\eta$ - $\omega$  curve disappeared as shear thinning phenomenon occurred. Moreover, the more ACL was added, the more pronounced the shear thinning became. The above phenomena was consistent with the changes in rheological properties of long-branched samples. Zero shear viscosity is the complex viscosity of a sample when the shear rate tends to zero and the system approaches an equilibrium state, which can reflect the characteristic structural of the sample in an equilibrium or near-equilibrium state. [16]For linear polymers, the zero shear viscosity is related to the relative molecular weight of the sample, and the relationship between the relative viscosity of PA6 and the relative molecular weight follows a power law of 3.4 [17](shown as Equation 2)

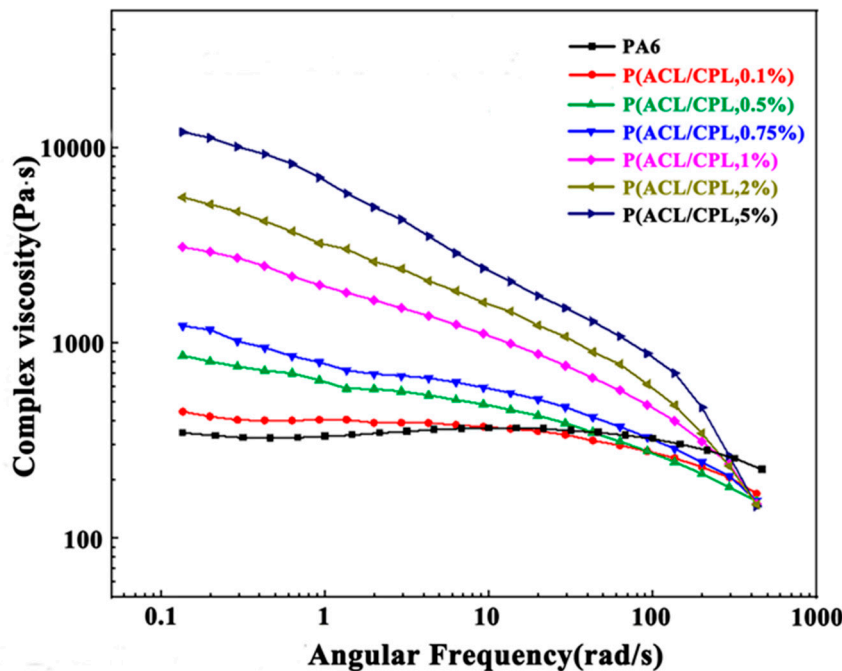


**Figure 4.** Complex viscosity of PA6 and P(ACL/CPL) co-polymers.

$$\eta_0 = kM_w^{3.4} \quad (2)$$

where  $\eta_0$  represents zero shear viscosity,  $M_w$  represents relative molecular weight, and  $k$  represents temperature-dependent constant. From the law, we can see that a larger zero shear viscosity corresponds to a higher molecular weight. However, with the addition of ACL, the molecular weight of the co-polymers first remains unchanged and then decreases. This indicates that the structure of the co-polymers is no longer linear. The zero shear viscosity of the co-polymers can be calculated through the simple Carreau equation with Cox-Merz rule[18]

$$\eta(\gamma)/\eta_0 = (1+(\gamma\tau_n)^2)^{(n-1)/2} \quad (3)$$

where  $\eta_0$  is the zero shear rate viscosity,  $\gamma$  is the shear rate,  $\tau_n$  is the characteristic time, and  $n$  is a parameter. From Table 1, we can see that after the addition of ACL exceeds 1wt%, the zero shear viscosity of the co-polymer increased significantly. This is because under near-equilibrium conditions, the viscosity of the material is mainly influenced by long branches with longer relaxation times. The entanglement of long branches hinders the movement of chain segments, resulting in an increase in zero shear viscosity of long-branched samples compared to linear chains with the same

molecular weight. In addition, due to the longer relaxation time corresponding to long branches, it means that it takes a lower deformation rate to fully relax them. Therefore, compared to linear chains with the same molecular weight, systems containing long branches start to exhibit a phenomenon of viscosity decrease at lower deformation rates, known as shear thinning phenomenon. [19–21,27] Generation of a gel structure can be another possible reason for the significant increase in zero shear viscosity. Though three dimensionally crosslinked polymers are incapable of macroscopic viscous flow, but the crosslinked chains can flow with other chains when the added amount of ACL is very small. However, it was checked that all co-polymer can completely soluble in formic acid with no remaining particles by the particle size analyzer. In addition, the crosslinked section is infusible in the melt, but the melt we observed in the experiment was all homogeneous[28].

**Table 1.** The basic properties of PA6 and P(ACL/CPL) co-polymers.

entry	feed CPL/ACL mass ratio	relative molecu larity	end group concentration amino/carboxyl (mmol/kg)	Melt Index	Zero shear viscosity (Pas)
1	0	2.524	16590	55.06/64.51	23.74
2	0.1/100	2.510	15850	59.06/65.98	32.58
3	0.5/100	2.486	15640	71.94/65.11	45.68
4	0.75/100	2.454	15220	83.48/66.26	44.32
5	1/100	2.424	14910	96.95/65.66	50.68
6	2/100	2.198	12280	153.4/77.26	92.42
7	5/100	1.897	9240	285.4/92.24	150.2

Storage modulus, loss modulus, and loss factor are also important rheological parameters reflecting the structure of the sample. The storage modulus reflects the elasticity of the sample, that is, the ability of the sample to maintain its original shape after being subjected to an external force, manifesting as solid-like behavior. The higher the storage modulus, the stronger the ability of the sample to maintain its original equilibrium state after being subjected to an external force, and the longer the time it takes to return to its original equilibrium shape after the same deformation, which can also be referred to as the relaxation time. On the other hand, the loss modulus reflects the viscous response of the sample, with a higher loss modulus indicating stronger liquid-like behavior.[22] According to linear viscoelastic theory, at the low-frequency region, pure linear PA6 exhibited terminal behavior, that is, the storage modulus and loss modulus have the following relationship with angular frequency: [23]

$$G' \propto \omega^2, \log G'' \propto 2\log\omega$$

$$G'' \propto \omega, \log G'' \propto \log\omega$$

According to the relationship, in the double logarithmic coordinate system, the slope of the linear pure PA6  $G'$ -  $\omega$  curve approaches 2 at low-frequency region. As shown in Figure 5(a), the slope of the PA6 curve was consistent with the above, while with the addition of cycloaliphatic lysine, the slope of the  $G'$ -  $\omega$  curve at the low-frequency region for our co-polymers gradually decreased from 1.75[P(ACL/CPL,0.1%)] to 0.17[P(ACL/CPL,5%)], deviating from the linear end behavior. Meanwhile, the storage modulus value increased by nearly 200 times, reflecting that with the addition of ACL, the long-chain branching structure in the co-polymers increased, the degree of molecular entanglement raised, and the sample's solid-like properties were enhanced, corresponding to a longer relaxation time.

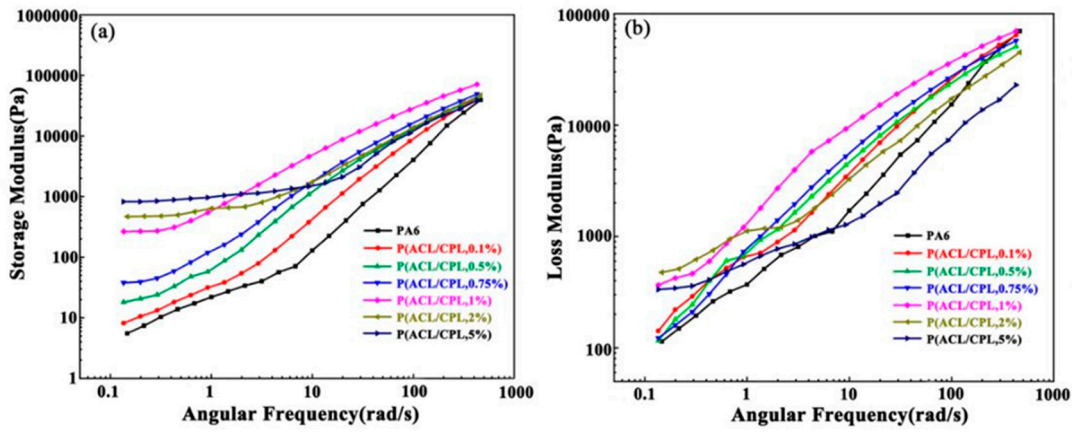


**Figure 5.** Storage modulus(a) and loss modulus(b) of PA6 and P(ACL/CPL) co-polymers.

The loss factor  $\tan\delta$  is the ratio of the loss modulus to the storage modulus ( $\tan\delta = G''/G'$ ), and its inverse trigonometric function is the loss angle. As the loss factor approaches zero, it indicates that the material is nearing purely elastic behavior while as the loss factor approaches infinity, it indicates that the material is nearing purely viscous behavior. The formation of branches is also reflected in the changes of the loss factor and loss angle. [24]Figure 6 shows the  $\tan\delta$ - $\omega$  curves for pure PA6 and our co-polymers with different contents of ACL. For pure PA6, the loss factor  $\tan\delta$  increased with the decrease of  $\omega$ , and the curve raise sharply at the low-frequency end, which was a typical liquid-like terminal behavior of linear molecular chains. With the addition of ACL, branched structure formed in the sample, and the  $\tan\delta$  decreased in the low-frequency region, with the curve beginning to show an inflection point. Moreover, as the co-polymerization amount of ACL increased, the  $\tan\delta$  continued to decrease, and the  $\tan\delta$ - $\omega$  curve gradually formed a plateau in the low-frequency region. This is consistent with the findings of Graebling et al. [25], who believed that the storage modulus of the sample is more sensitive to the formation of branches, and a small amount of branching can cause a significant increase in the storage modulus, while the loss modulus is less sensitive to this, hence the magnitude of  $\tan\delta$  is mainly influenced by the changes in the storage modulus. With the formation of branches, there is a significant increase in the storage modulus in the low-frequency region, while the change in the loss modulus is relatively small, therefore  $\tan\delta$  begins to decline in the low-frequency region At the same time, the presence of branches enhances the relaxation time of the sample at the low-frequency end, and the storage modulus of the sample gradually stabilizes, hence the  $\tan\delta$ - $\omega$  curve shows a plateau.

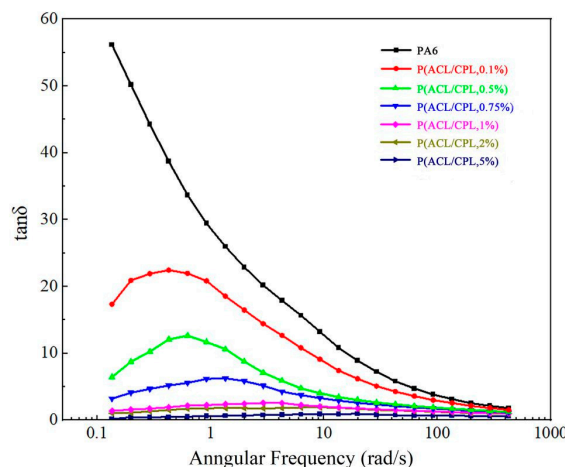


**Figure 6.** Loss factor of PA6 and P(ACL/CPL) co-polymers.

The Cole-Cole plot is a graph that represents the relationship between the imaginary viscosity  $\eta''$  ( $\eta'' = G'/\omega$ ) and the real viscosity  $\eta'$  ( $\eta' = G''/\omega$ ) of a sample. The deflection of the Cole-Cole plot curve can be used to characterize the relaxation time and relaxation mechanism of polymer samples. [26] For samples with linear molecular chain structures, their Cole-Cole curves are close to semicircular. In Figure 7, the Cole-Cole curve of PA6 is close to semicircular, which is consistent with the conclusion. With the generation of branches, the Cole-Cole curve of the N-PA6 sample gradually deviates from the semicircular shape, and the curve begins to turn up at high  $\eta'$ , that is, in the low-frequency region, indicating that the relaxation process of the sample is extended, the relaxation time of the system increases, and the greater the amount of co-polymerized ACL, the greater the semicircular deflection of the corresponding curve, with more branched structures corresponding to longer relaxation times.

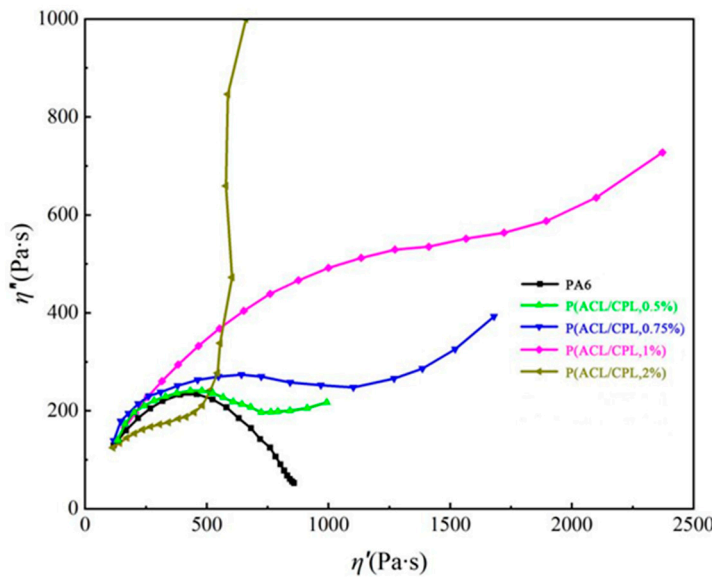


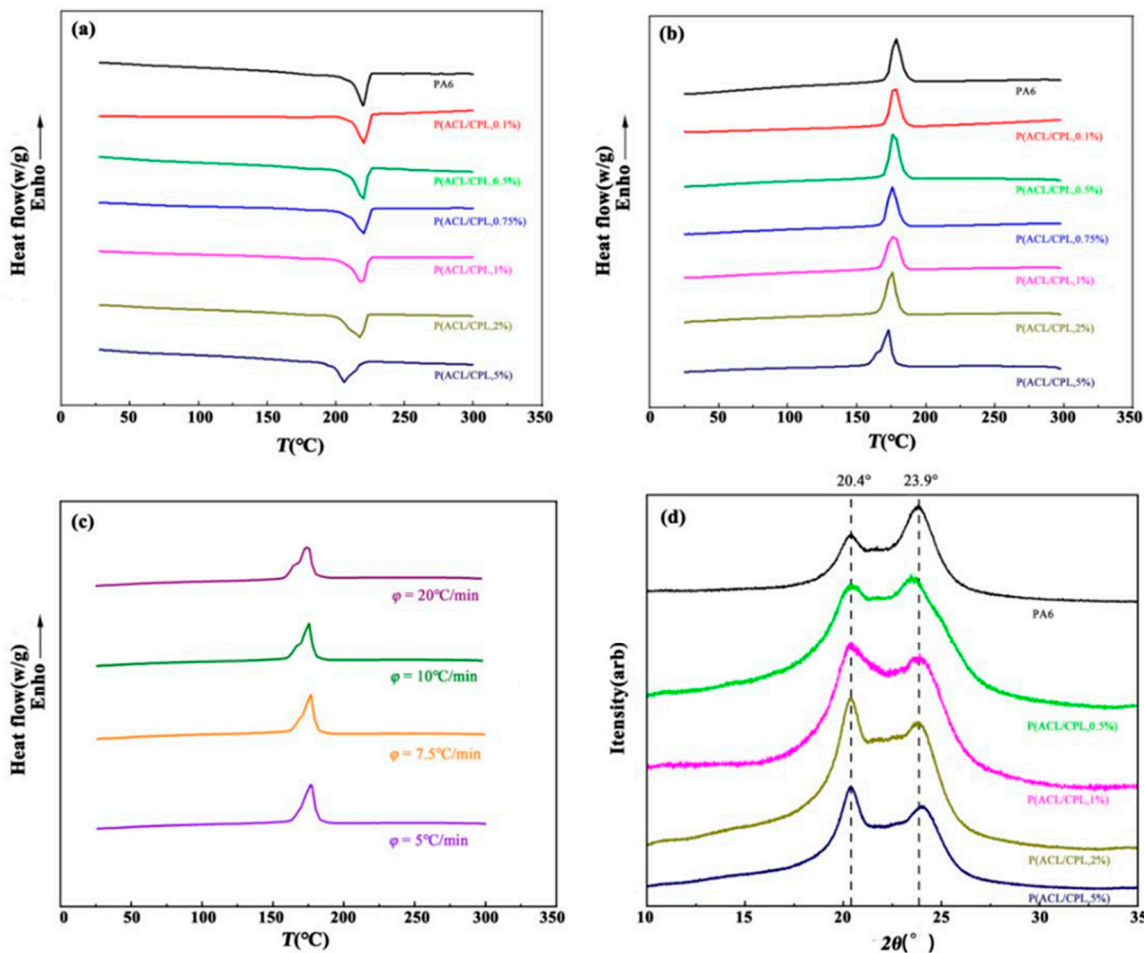
**Figure 7.** Cole-cole figure of PA6 and P(ACL/CPL) co-polymers.

The end-group test results of the co-polymers are shown in Table 1. When the amount of ACL was less than 1%, the carboxyl group concentration was similar, around 65mmol/kg. When the amount of ACL exceeded 1%, the carboxyl group concentration increased, which was due to a significant decrease in molecular weight. The end-amine concentration of the copolymer significantly increased with the addition of ACL, as well as the ratio of end-amine to end-carboxyl groups. Based on the mechanism of branching mentioned above, this is because the addition of ACL increases the number of branches, and each branch end is also an amino group, resulting in a significant increase in amino group concentration.

The thermal properties of the co-polymers were determined by DSC scanning, as shown in Figure 8(a)(b) and Table 2. It can be seen that the melting point of the samples significantly decreases when the amount of ACL exceeds 1wt%. The crystallization process of the samples is more sensitive to the addition of ACL, as the crystallization temperature and degree of crystallinity decrease significantly, and the crystallization peak becomes broader. This is because the addition of a small amount of ACL disrupts the regularity of the molecular chains, and the presence of some shorter side chains reduced the chain migration rate, hindering the crystallization of the samples [30].

**Table 2.** The thermal properties of PA6 and P(ACL/CPL) co-polymers.

entry	feed CPL/ACLmass ratio	Melting point(°C)	crystallization temperature(°C)	Crystallinity (%)
1	0	221.00	184.02	27.38
2	0.1/100	220.57	177.13	25.59
3	0.5/100	219.63	176.07	25.56
4	0.75/100	219.06	175.32	25.32
5	1/100	218.82	175.69	25.19
6	2/100	216.67	174.88	24.20
7	5/100	206.24	172.28	22.56

**Figure 8.** (a):Melting curves of PA6 and P(ACL/CPL) co-polymers (b):Crystallization curves of PA6 and P(ACL/CPL) co-polymers (c):Crystallization of P(ACL/CPL,5%) in different cooling rate (d):.XRD spectra of PA6 and P(ACL/CPL) co-polymers.

When the ACL content is 5%, the co-polymer exhibited a double crystallization peak, which may be due to different crystallization temperatures of different segments in the copolymer, or the presence of more side chains and network structures in the polymer, under the cooling rate of 10°C/min, the molecular chains responded insufficiently, resulting in incomplete folding and

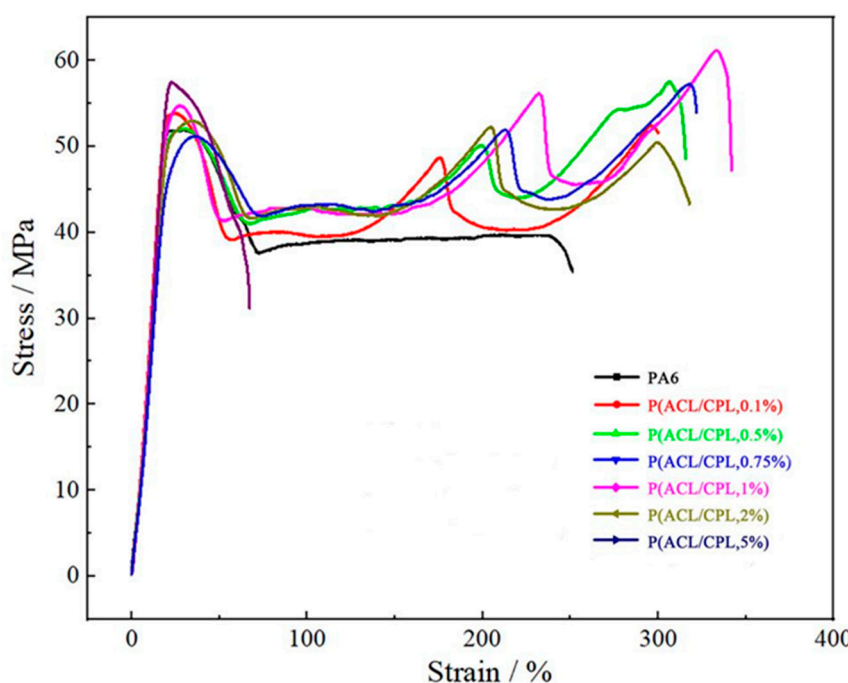
arrangement of the molecular chains, leading to different crystalline forms. [31]Therefore, we conducted cooling crystallization tests on the co-polymers at different cooling rates, and the cooling curves obtained are shown in Figure 8(c). The double crystallization peak becomes more pronounced when the cooling rate is increased to 20°C/min, while the crystallization peak becomes a single peak when the cooling rate is reduced to 5°C/min. This indicates that the double peaks observed in the cooling crystallization curve at higher cooling rates are due to the slow response of the molecular chains to the fast cooling rate, and the difference in crystallization temperature of different side chains in the sample is not significant.

Figure 8(d) shows the X-ray diffraction characterization results of the copolymers with different ACL contents. It can be seen that although the addition of ACL affects the crystallinity of the samples, the crystal structure of the samples remained unchanged, and all samples exhibit characteristic peaks at 20.4° and 23.9°, corresponding to the  $\alpha$ -crystal form of nylon 6.

**Table 3.** The tensile mechanical properties of PA6 and P(ACL/CPL) co-polymers.

entry	feed CPL/ACLmass ratio	yield strength (MPa)	tensile strength (MPa)	fracture elongation rate (%)
1	0	51.55	42.52	250.24
2	0.1/100	51.93	50.12	300.02
3	0.5/100	52.07	55.42	312.24
4	0.75/100	52.66	58.84	318.27
5	1/100	52.87	62.27	358.24
6	2/100	54.25	51.92	320.52
7	5/100	58.20	58.20	66.67

Figure 9 shows the stress-strain curve during the tensile process of co-polymers with different ACL contents. It can be seen that the stress decreased after the yield point of pure nylon samples, and then remained constant until the sample fractures, which was the tensile strength. With the addition of ACL, the stress plateau after yield became shorter, and then increases with strain, experiencing 2-4 times increment. When the ACL content did not exceed 1wt%, the tensile strength of the samples increased with the ACL content, and was always greater than the yield strength, indicating the occurrence of strain hardening. When the ACL content was 2%, the stress after yield also increased multiple times with strain, but the ultimate fracture strength was lower than the yield strength, indicating no strain hardening phenomenon. When the ACL content was 5%, the sample fractured quickly after yield. With the addition of ACL, the change in co-polymers yield strength was not significant, but the tensile strength and fracture elongation rate significantly increased when the ACL content was below 1wt%, indicating enhanced toughness of the samples. After the ACL content exceeded 1wt%, the tensile strength and fracture elongation rate decreased. Typically, for linear polymers, the tensile strength and fracture elongation rate decreased with decreasing crystallinity. The addition of ACL reduced the crystallinity but increased the branching, resulting in more chain entanglements. During the tensile process, the entangled chains rearrange and gradually untangled after yield, requiring further energy barrier overcoming, thus the stress gradually increased. [32]When the ACL content exceeded 2%, the molecular weight of the co-polymers started to decrease significantly, leading to a decrease in the subsequent tensile strength and fracture elongation rate. Comparing the tensile properties of co-polymers with different ACL contents, P(ACL/CPL,1%) exhibited the best tensile mechanical properties.



**Figure 9.** Tensile curve of PA6 and P(ACL/CPL) co-polymers.

#### 4. Conclusions

In this study, we successfully synthesized a novel branched polyamide 6[P(ACL/CPL)] with  $\epsilon$ -caprolactam(CPL) and  $\alpha$ -Amino- $\epsilon$ -caprolactam(ACL) through hydrolytic ring-open co-polymerization. The branched chain structure caused a remarkable enhancement in the rheological properties. The met index(MFR),zero shear rate viscosity and storage modulus at low frequency region had a remarkable increase. The shear thinning phenomenon became more obvious. The melting point and crystallinity of co-polymers decreased with the increase of ACL addition. However, the crystal structure of the samples remained unchanged. The appropriate addition amount of ACL can improve the tensile mechanical properties of the co-polymers. When the amount of ACL is 1%, the tensile strength and fracture elongation rate of the co-polymers had the most significant increase.

**Data Availability Statement:** Data are contained within the article.

**Acknowledgments:** The authors would like to thank the support from the Major Program Foundation of SINOPEC.

#### References

1. M.I. Kohan. *Nylon plastics handbook*; Hanser: New York, USA, 1995; pp. 112-118.
2. Y. Gong, A. Liu, G. Yang. Polyamide single polymer composites prepared via in situ anionic polymerization of  $\epsilon$ -caprolactam. *Compos. Part. A Appl. Sci. Manuf* **2010**, *41*, 1006–1011.
3. K. Hashimoto. Ring-opening polymerization of lactams. Living anionic polymerization and its applications. *Prog. Polym. Sci.* **2000**, *25*, 1411–1462.
4. S. Zhang, Y. Wu, H. Yang, P. Ji, C. Wang, H. Wang, Z. Yan. Preparing Cationic Dyeable Polyamide 6 Filaments by Combining the Masterbatch Technique with Melt Copolymerization. *Text. Res. J.* **2022**, *511–524*.
5. M. Xu, H. Yan, Q. He, C. Wan, T. Liu, L. Zhao, C.B. Park. Chain extension of polyamide 6 using multifunctional chain extenders and reactive extrusion for melt foaming. *Eur. Polym.* **2017**, *96*, 210–220.
6. S. Yilmaz, O. Gul, T. Yilmaz. Effect of chain extender and terpolymers on tensile and fracture properties of polyamide 6. *Polymer* **2015**, *65*, 63–71.
7. S. H. Tabatabaei, P. J. Carreau, A. Ajji. Rheological and thermal properties of blends of a long-chain branched polypropylene and different linear polypropylenes. *Chem Eng Sci* **2009**, *64*, 4719–4731.
8. T. Huber, P. Pötschke, G. Pompe, et al. Blends of hyper-branched poly(ether amide)s and polyamide-6. *Macromol. Mater Eng* **2000**, *280/281*, 33–40.

9. J. Chen, Y. Dong, C. Xiao, Y. Tao, X. Wang. Organocatalyzed Ring-Opening Polymerization of Cyclic Lysine Derivative: Sustainable Access to Cationic Poly( $\epsilon$ -lysine) Mimics. *Macromolecules* **2021**, *54*, 2226–2231.
10. M. Scholl, Z. Kadlecova. Controlling Polymer Architecture in the Thermal Hyperbranched Polymerization of L-Lysine. *Macromolecules* **2007**, *40*, 5726–5734.
11. P. Steeman, A. Nijenhuis. The effect of random branching on the balance between flow and mechanical properties of polyamide 6. *Polymer* **2010**, *51*, 2700–2707.
12. J. Li, J. Song, W. Ji, L. Zhang, T. Zhang. Preparation and properties of branched copolymerized polyamide 6. *PETROCHEMICAL TECHNOLOGY* **2019**, *48*, 938–942.
13. K. Liu, B. Shao, H. Liu, J. He, J.; A. Zheng, G. Li, B. Zheng, Z. Li, W. Liu, X. Li, B. Zong. Sustainable production of dimethyl-protected cyclic lysine over Pd/m-Al<sub>2</sub>O<sub>3</sub>-Si catalysts and its application in synthesis of antibacterial nylon6 copolymers. *Chem. Eng. J.* **2023**, *463*, 142504.
14. P.G. Gallen, Nylon 6, in: J.E. Mark (Ed..) *Polymer Data Handbook*, Oxford University Press, New York, 1999, pp. 180–185.
15. M. Sugimoto, T. Tanaka, Y. Masubuchi. Effect of chain structure on the melt rheology of modified polypropylene. *J. Appl. Polym. Sci.* **1999**, *73*, 1493–1500.
16. H. Kima, K. Oha, Y. Seo. Rheological and mechanical properties of a novel polyamide 6 synthesized by anionic polymerization of  $\epsilon$ -caprolactam in a twin-screw extruder. *Polymer* **2019**, *177*, 196–201.
17. M. Doi. Explanation for the 3.4-power law for viscosity of polymeric liquids on the basis of the tube model. *J. Polym. Sci. B* **1983**, *21*, 667–684.
18. Y.P. Seo. Effect of molecular structure change on the melt rheological properties of a polyamide (nylon 6). *ACS Omega* **2018**, *12*, 16549–16555.
19. A. D. Gotsis, B. L. F. Zeevenhoven, C. Tsenoglou. Effect of long branches on the rheology of polypropylene. *Journal of Rheology* **2004**, *48*, 895–914.
20. Z. Zhang, D. Wan, H. Xing Haiping, et al. The effect of tetramethylthiuram disulfide on the heat-induction melt-grafting of polypropylene. *Chinese Journal of Applied Chemistry* **2011**, *28*, 1130–1134.
21. F. Su, H. Huang, Y. Zou. Rheological behavior and thermal properties of long chain branching polypropylene prepared by reactive extrusion. *China Plastics*, **2009**, *23*, 31–34.
22. E. Kolodka, W. Wang, S. Zhu. Copolymerization of propylene with poly(ethylene-CO-propylene) macromonomer and branch chain-length dependence of rheological properties. *Macromolecules* **2002**, *35*, 10062–10070.
23. M. Rubinstein, R.H. Colby, *Polymer Physics*, first ed., Oxford University Press, New York, 2003, pp.363–367.
24. Robertson C G, Franco C Q, Srinivas S. Extent of branching from linear viscoelasticity of long-chain-branched polymers. *J. Polym. Sci. Part B: Polymer Physics* **2004**, *42*, 1671–1684.
25. D. Graebling. Synthesis of branched polypropylene by a reactive extrusion process. *Macromolecules* **2002**, *35*, 4602–4610.
26. S. Havriliak, S. Negam. A complex plane representation of dielectric and mechanical relaxation processes in some polymers. *Polymer* **1967**, *8*, 161–210.
27. C. Kun, H. Jin, Z. Qiaoling, M. Zhi. New progress in analysis and characterization of long chain branched structure in high melt strength polypropylene. *Chemical Industry and Engineering Progress* **2022**, *41*, 5425–5440.
28. R.J. Young, P.A. Lovell. *Introduction to Polymers*; CRC Press: Boca Raton, USA, 2011, pp.263–265.
29. Ch. A. Kruissink, G. M. van der Want, A. J. Staverman. On the Mechanism of the Polymerization of  $\epsilon$ -Caprolactam. I. The Polymerization Initiated by  $\epsilon$ -Aminocaproic Acid. *JOURNAL OF POLYMER SCIENCE* **1958**, *6*, 67–80.
30. E. Núñez, C. Ferrando, E. Malmström, H. Claesson, U.W. Gedde. Crystallization behavior and morphology of star polyesters with poly( $\epsilon$ -caprolactone) arms. *J. Macromol. Sci. B* **2004**, *43*, 1143–1160.
31. L.Y. And, W.A. Goddard III. Nylon 6 crystal structures, folds and lamellae from theory. *Macromolecules* **2002**, *35*, 8440–8455.
32. D. Bin, W. Junqi, C. Shangtao, Z. Fengbo, Z. Wenqin. Extensional Rheological Behavior of Long Chain Branched PP. *Plastics Science and Technology* **2020**, *48*, 8–51.

**Disclaimer/Publisher's Note:** The statements, opinions and data contained in all publications are solely those of the individual author(s) and contributor(s) and not of MDPI and/or the editor(s). MDPI and/or the editor(s) disclaim responsibility for any injury to people or property resulting from any ideas, methods, instructions or products referred to in the content.